Title	Scalable production of silicon nanocone solar cells in integrated plasma photovoltaic nanofabrication cluster
Author(s)	Shiyong Huang, Jian Wei Mark Lim, Chia Sern Chan, Shuyan Xu, Deyuan Wei, Yingnan Guo, Luxiang Xu and Kostya (Ken) Ostrikov
Source	*Plasma Processes and Polymers, 13*(1), 161-169 http://dx.doi.org/10.1002/ppap.201500086
Published by	Wiley-VCH Verlag

Plasma Processes and Polymers

Scalable Production of Silicon Nanocone Solar Cells in Integrated Plasma Photovoltaic Nanofabrication Cluster

Journal:	*Plasma Processes and Polymers*
Manuscript ID:	Draft
Wiley - Manuscript type:	Full Paper
Date Submitted by the Author:	n/a
Complete List of Authors:	Huang, Shiyong; Plasma Sources and Applications Centre (PSAC), National Institute of Education, Nanyang Technological University, Natural Sciences and Science Education (NSSE) Lim, Jian Wei Mark; Plasma Sources and Applications Centre (PSAC), National Institute of Education, Nanyang Technological University, Natural Sciences and Science Education (NSSE) Chan, Chia Sern; Plasma Sources and Applications Centre (PSAC), National Institute of Education, Nanyang Technological University, Natural Sciences and Science Education (NSSE) Xu, Shuyan; Plasma Sources and Applications Centre (PSAC), National Institute of Education, Nanyang Technological University, Natural Sciences and Science Education (NSSE) Wei, Deyuan; Plasma Sources and Applications Centre (PSAC), National Institute of Education, Nanyang Technological University, Natural Sciences and Science Education (NSSE) Guo, Yingnan; Plasma Sources and Applications Centre (PSAC), National Institute of Education, Nanyang Technological University, Natural Sciences and Science Education (NSSE) Xu, Luxiang; Plasma Sources and Applications Centre (PSAC), National Institute of Education, Nanyang Technological University, Natural Sciences and Science Education (NSSE) Ostrikov, Kostya; CSIRO, Manufacturing Flagship
Keywords:	

Scalable Production of Silicon Nanocone Solar Cells in Integrated Plasma Photovoltaic Nanofabrication Cluster

Shiyong Huang, Lim Jian Wei Mark, Chia Sern Chan, Shuyan Xu, Deyuan Wei, Yingnan Guo, Luxiang Xu, Kostya (Ken) Ostrikov

Dr. S. Y. Huang, Mr. J. W. M. Lim, Dr. C. S. Chan, Prof. S. Xu, Dr. D. Y. Wei, Mr. Y. N. Guo, Mr. L. X. Xu
Plasma Sources and Applications Center (PSAC), NIE, Nanyang Technological University, 1 Nanyang Walk, 637616, Singapore
E-mail: shuyan.xu@nie.edu.sg

Prof. Kostya (Ken) Ostrikov
Plasma Nanoscience Laboratories, Industrial Innovation, CSIRO Manufacturing Flagship, P.O. Box 218, Lindfield NSW 2070, Australia
E-mail: kostya.ostrikov@csiro.au

Prof. Kostya (Ken) Ostrikov
Institute for Future Environments and School of Chemistry, Physics, and Mechanical Engineering, Queensland University of Technology, Brisbane, QLD 4000, Australia
E-mail: kostya.ostrikov@qut.edu.au

Surface texturing is a method widely adopted by industries to reduce the reflective losses in photovoltaic (PV) cells. In this work, a multi-chambered Integrated Plasma Photovoltaic Nanofabrication Cluster facility was used to produce nanocone surface textured polycrystalline (PX) PV cells. An inductively coupled plasma (ICP) discharge of O_2 and SF_6 was used to remove damage on PX p-type silicon wafers. Following that, a mixture of H_2 and Ar plasma was used to texture an anti-reflecting array of silicon nanocones on the surface, while simultaneously forming a p-n junction. A plasma enhanced chemical vapour deposition (PECVD) process was utilized using SiH_4, CO_2, N_2 and H_2 precursors for front and back surface passivation for growth of SiN_x:H and SiO_xH thin films. Aluminium electrodes were sputtered on using an RF magnetron sputtering facility to provide the contacts for the PV cell. Scanning electron microscopy of textured sample surfaces revealed uniform, well defined, high aspect ratio nanocones. The absorption spectra of the resulting surface show dramatic reductions in the reflectance of the wafers, and external quantum efficiency measurements show improved spectral response for the 300 nm – 1100 nm region. The resulting cells showed promising photovoltaic responses, with short circuit-currents of 36 mA/cm^2, open circuit voltages of 560 mV, fill factors reaching 80% and conversion efficiencies of up to 14.8%. The feedstock gases utilized in this entire process were mostly environmentally friendly, and the single plasma based processing cluster eliminated the need for excessive waste generated from chemicals that would be otherwise found in commercial production lines. This work shows exciting potential in the pursuit of fabricating low cost, environmentally friendly and highly efficient PV modules to address the problems posed by the global energy crisis.

1. Introduction

Throughout the last decade, the renewable energy market has been dominated primarily by silicon photovoltaic (PV) modules.[1, 2] Silicon based PV modules account for more than 80% of the solar cells being utilized globally. Even though the cost of fabrication and implementation of PV modules have been drastically reduced over the years due to intensive research in the field and a revived interest in renewable energy to alleviate the effects of an impending global energy crisis, silicon PV modules are still relatively expensive.[3]

As such, cost still remains a major hurdle that needs to be overcome in order to realize the widespread implementation of PV cells harnessing solar energy. Hence, it is of major interest to many industries and research institutions to develop alternative and novel fabrication methods as well as solid state semiconductors that offer the potential to reduce production costs associated with conventional silicon PV cells as well as to eliminate the emission of toxic byproducts that are inherent with conventional fabrication methods.

Polycrystalline (PX) silicon based PV cells is the most common type of commercially available solar cells.[4, 5] The reason behind the success of PX silicon based modules is in its ability to meet the requirements for a PV cell that could be scaled up in modules to be implemented in large scaled grids. The public's reception to PX PV cells has been overwhelming over the years due to their low cost of fabrication, and the reliability in large-scale PV modules which are simple in design and are easily manufactured through the established industrial process flow.

Silicon is also known to be the most mature PV material, with its applications widely studied and developed by many research institutes and companies, which eventually drives the costs for producing

high quality materials down over the years.[6] As such, even though the efficiency of PX silicon based PV cells have been known to be relatively lower than its next generation counterparts, a large majority of commercial PV panels are still PX based, due to the technology and raw materials required being readily available for mass production. Apart from the cost of production, PX silicon is also non-toxic as a material, making it truly an environmentally friendly alternative source of energy in terms of its ability to be replenished rapidly and its minimal negative effects on the environment.[3]

Primarily, a good PV cell has to have reasonably high power conversion efficiency. To meet that demand, the cell has to minimize optical losses by ensuring as much of the incident light can be harnessed to give rise to a significant photo-current. This could be done by minimizing the reflective losses on the surface of the PV cell through texturing, and by employing anti-reflective coatings for light management.[7, 8]

The PV cell must also possess a good, high quality p-n junction to ensure that charge-carriers are rapidly swept to the different layers of the cell before recombination takes place. A quality p-n junction enhances carrier transport while increasing the lifetime of the charge-carriers in the PV cell. To be considered as a commercially viable renewable source of energy, fabrication of PV cells should be low cost (economical starting materials and reagents), as well as simple, with a minimized number of sophisticated processing steps with results which can be reproduced reliably.

One of the most persistent problems that researchers face while fabricating PV cells would be the production of a high quality p-n junction.[9, 10] Conventional methods of junction formation commonly employ the diffusion of dopant atoms through thermal or chemical diffusion processes. These processing methods are hard to control, and it is a challenge to tailor the junction depth or dopant concentration to a great level of precision for various applications.[11, 12] On top of that, prior to processing, wafers are required to be cleaned with copious amounts of acids in an intricate cleaning process,[13, 14] and large

amounts of the processing costs would be borne on chemicals and water used for rinsing of substrates post and during processing, bearing in mind that the wastes incurred also bring about negative environmental impacts.

Recently, plasmas have proven to be effective in reducing the number of processing steps in the dry fabrication of PV cells.[15-17] Most notably, a dry processing technique has proven successful in etching an anti-reflecting array of silicon nanocones on the surface of a substrate, while simultaneously forming a p-n junction in the process.[18, 19]

Here we demonstrate an advanced process of fabricating PX PV cells which have enhanced power conversion efficiencies (PCE). The fabrication process relies on relatively cheap materials and feedstocks which bear minimal negative environmental impact during fabrication. In this work, a multi-chambered plasma processing cluster was developed to fabricate PX silicon PV cells. The entire fabrication process took place in a controlled vacuum environment of the Integrated Plasma Photovoltaic Nanofabrication Cluster (IPPNC) to minimize contamination from the ambient which is vital in producing device grade PV materials. The entire PV fabrication process comprises the four main steps, each taking place in a different chamber in the cluster.

2. Experimental methodology

A plasma cleaning step using the LF-ICP discharge in O_2 and SF_6 gases was performed in the first chamber which removed the saw damage as opposed to the conventional wet chemical etching methods for damage removal on the silicon substrate. The advantage of dry plasma processing eliminates the requirement for large volumes of chemicals and other sources of waste due to extensive rinsing to achieve

high purity silicon for PV applications.

The next step involves plasma etching with Ar and H_2 feedstocks which textured high aspect ratio nanocones onto the surface of the silicon wafer which reduced reflective losses. While texturing silicon nanocones onto the surface to reduce reflectivity, the exposure of the silicon wafer to the Ar and H_2 discharge also simultaneously resulted in a conductivity type conversion,[18-20] forming a high quality p-n junction in the process, providing an emitter layer which is essential in a PV cell.

Afterwards, a CCP magnetron sputtering facility was employed to deposit aluminium electrodes as contacts for the PV cell. A final ICP assisted chemical vapour deposition (CVD) step was used in the final chamber with SiH_4, N_2, O_2 and H_2 as feedstocks for growth of SiN_x:H and SiO_x:H films for surface passivation.[21, 22]

The resulting PV cells were found to have high aspect ratio silicon nanocones textured on the surface, with a huge reduction in reflectivity giving rise to black silicon appearance. Most importantly, the external quantum efficiencies of the resulting PV cells were found to have improved through the various processing stages, indicating the effectiveness of each step and the compatibility for each method to be put together in an integrated multi-chambered PV cell plasma processing cluster.

Commercial boron-doped p-type polycrystalline silicon wafers were used as substrates in this work. The substrates were placed in a loading chamber in the IPPNC before being pushed into a larger distribution chamber with the aid of sample loading rods. The IPPNC fabrication cluster was evacuated by a 2-stage rotary and turbomolecular pump suite to achieve a base pressure of $<10^{-4}$ Pa. Each processing chamber in the IPPNC is separated by an automatic electronically triggered gate which isolates each chamber, minimizing the effects of cross contamination from feedstocks and byproducts as the substrate is

transferred from 1 chamber to another as shown in figure 1 (b).

The distribution chamber of the IPPNC is linked to 4 processing chambers, each of which serves a different function in the treatment of the PX Si wafers. All processing chambers are fitted with gas inlets which introduce working gases into the reaction chambers. The gas flux is controlled with the MKS 1100 mass flow controllers, and the base pressure can be varied using a valve which varies the outlets which lead to the vacuum pumps. The chambers also feature elevated substrate holders which enable samples to be mounted and transferred from one chamber to the next easily, and have heating elements attached for provision of heating during certain processes. The substrate holders are also connected to an external voltage supply to provide a variable bias on the substrate holder. All processing chambers were cylindrical in geometry, and have double stainless steel walls to enable coolants to circulate within. Portholes align the cylindrical chamber radially that enable various diagnostic probes to be positioned close to the discharge.

Samples were first transferred from the distribution chamber to the first plasma processing chamber in the cluster (ICP 1), which is configured as an inductively coupled plasma reactor. A planar RF coil lies on top of the reaction chamber which is sealed with a dielectric lid and a Viton O-ring. An RF power generator supplies 568 kHz of RF power through a matching network as the feedstock gases of O_2 and SF_6 are introduced from the gas inlets. Plasma reactive ion etching for removal of saw damage was conducted with a supplied power of 1.7 kW of input power and -50 V of bias supplied to the substrate holder. The pressure of the discharge was held at 2.0 Pa, and the ratio of O_2 to SF_6 was varied with the aid of mass flow controllers to determine the optimum conditions for plasma cleaning for removal of saw damage. The surface morphology of samples post processing and the etch rate were investigated through scanning electron microscopy (SEM) with a JEOL JSM 6700F field emission SEM.

Samples were then transferred to the neighboring ICP chamber (ICP 2) which is identical in configuration with ICP 1, with the exception of the gas inlets which supply Ar and H_2 feedstock gases. In this chamber, a plasma discharge of Ar + H_2 was maintained to etch an array of silicon nanocones on the surface of the substrate to reduce reflective losses, as well as to simultaneously form an emitter layer through p-n junction formation during the surface texturing process. The discharge was maintained at a pressure of 1.7 Pa, with the ratio of Ar : H_2 = 1.2 : 14.4.

With the aid of a heating element, the temperature of the substrate was raised to 500 ºC, and the RF power supplied by the generator was kept at 2.0 kW for the entire processing duration of 30 minutes. To deduce the effectiveness and extent of the treated surface, samples were characterized using Scanning Electron Microscopy (SEM) to determine the aspect ratio and distribution of the nanostructures. The reduction in reflective losses was quantified by obtaining the reflectance spectra of the samples with a Zolix SCS10-X150-DSSC UV-Vis spectrometer with an integrating sphere.

To form the electrical contacts of the PV cell, the samples were then transferred into an RF (13.56 MHz) magnetron sputtering facility in the next chamber. An aluminium disc was used as a target and was placed 80 mm above the substrates. Sputtering was done with the aid of a pure Ar discharge maintained at 1.0 Pa, and an input power of 240W. The temperature in the chamber was raised to 250 ºC with the attached heating element. The substrates were shielded with a mask during the first 10 minutes of discharge to allow the removal of contaminant species from the target and the chamber, while allowing for the plasma sputtering conditions to stabilize. The substrates were exposed to the discharge for 5 minutes for the deposition of the contacts for the PV cell.

At the final stage of dry processing in the fabrication cluster, substrates were transferred into an ICP reactor for plasma assisted chemical vapour deposition (CVD) of silicon nitride for surface passivation.

Surface passivation terminates the dangling bonds present on the surface of PX silicon. If these bonds are left unpassivated, they will serve as recombination centers which reduce the lifetime of the photo-generated carriers in the PV cell, affecting both the short-circuit current, open-circuit voltage and power conversion efficiency as a result.

The ICP CVD passivation process employed SiH_4, N_2 and H_2 gasses as feedstocks in a 1:2:1 ratio held at 5.0 Pa. The samples were exposed to the discharge for 5 minutes. After processing in the cluster, samples were then removed and placed in a furnace for thermal annealing in N_2 ambient at 250 ºC for 60 minutes. Samples were characterized with SEM to gain insights on the surface morphology and etch rates, and the external quantum efficiencies (EQE) with reflectance spectra were obtained to quantify the effectiveness of each process in the plasma fabrication cluster.

3. Results and Discussion

Figure 2(a) shows the surface morphology via SEM, of an untreated PX Si wafer after being cut into an appropriate size for processing. The saw damage from cutting is evident and is undesirable for production of device grade materials. Figures 2 (b) and (c) are 45 º tilted images obtained through SEM of samples which were subjected to an SF_6 + O_2 plasma discharge for removal of saw damage in ICP 1 using different gas ratios of 6%, and 16% of oxygen, respectively.

The optimum gas ratio was found to be 16% of oxygen. This is due to the etching-rate limiting condition being dependent on desorption of SiF_4 molecules in the SF_6 + O_2 plasma. It is understood that oxygen has a dual role in plasma etching processes which utilize gaseous halide feedstock.[23, 24] This explains the profiles obtained in figures 2 (b) and (c). Oxygen reacts with fluorine containing species in the plasma (in

this case, SF_6) to liberate fluorine which acts as the etchant in this process. With a relatively low ratio of oxygen supplied to the reaction chamber, the production of etchants induced by oxygen species in the plasma is not optimum, and hence the etch rate is severely affected.

This results in the profiles seen in figure 2 (b) showing a slight amount of saw damage removal, leaving behind small regions where the etch process was insufficient in smoothening out damage. As the oxygen ratio was increased from 6 % to 16 % as can be seen in the SEM profile in figure 2 (c), an optimum etch recipe was realised as complete saw damage removal was achieved from this condition.

Further increasing the oxygen ratio resulted in profiles which were rougher and had residual saw damage present on the surface. This is due to the dual role that oxygen serves in this etch process. While oxygen is a necessary precursor for production of the etchant (fluorine), oxygen also competes for adsorption sites on silicon with fluorine. An excess of oxygen in the discharge would consequently not increase the etch rate but conversely have a negative effect on the etch efficiency as it slows down the etching process by adsorbing onto active silicon sites.

This can be seen in the SEM profiles of samples which were etched with an excess of oxygen above the optimal condition, resulting in a poorly treated surface, due to the decreased etch rate as mentioned beforehand. This observation is also illustrated in figure 2 (d), which shows how the etch rate initially increases with increasing oxygen ratio up to an optimum value of 16 % before a reverse trend is seen, with the etch rate decreasing with additional increase of oxygen by volume.

Dry processing in ICP 2 etched silicon nanocones onto the surface of the silicon substrates, while simultaneously causing a p-to-n type conductivity conversion (PNTCC) in the wafers due to a p-n junction formation. In a single process, a textured emitter layer was formed with high aspect ratio silicon

nanocones with low reflectivity, indicating the production of a black silicon (b-Si) surface. Figures 3 (a) – (d) show the SEM profiles of b-Si formed through Ar + H_2 etching of silicon with different Ar and H_2 ratios.

To fabricate an ideal material with low reflective losses it was of paramount importance to increase the average density of the nanostructures textured onto the surface as well as to increase the aspect (height – to – full width at half maximum, H-FWHM) ratio of the anti-reflection arrays. This was done through manipulation of the applied bias, supplied RF power, temperature of the chamber and the Ar + H_2 mass flow ratio.

It was found that high density ultra-low reflectivity b-Si could be obtained with relatively high aspect ratios and commendable open-circuit voltages (V_{oc}) which was obtained through a Sinton instruments WCT-120 Suns-Voc measurement stage. The aspect ratios of the silicon nanocones were found to have increased with an increasing H_2/Ar ratio. Figure 3 (a) shows the tiny nanocones etched on a substrate with 0.10 H_2/Ar ratio. As the ratio was increased to 0.20 and 0.30, the morphology changes as shown in Figures 3 (b) and (c), respectively. The H-FWHM of the nanocones was seen to increase as well. When the H_2/Ar ratio was 0.40, the etched profile of the silicon nanocones as seen in Figure 3 (d), was determined to be the best for reducing reflectivity losses as seen from its high H-FWHM of 1:5. The etched nanocones obtained under all the mentioned process conditions were found to be very densely packed (exhibiting surface densities of ~10^{10} cm^{-2}).

The reflectivity of the textured wafers was measured with the aid of an Zolix SCS10-X150-DSSC UV-Vis spectrometer with an integrating sphere (Zolix SCS QE-C2). The reflectance spectra of the samples are shown in Figure 4 (b). The average reflectivity of samples which were subjected to SF_6 + O_2 plasma for removal of saw damage only was found to be around 30%. However, after etching of the nanocones onto

the surface, the reflectivity of the samples were found to have decreased drastically to less than 2% (b-Si). The reflectivity was found to have increased with the increased aspect ratio.

At the same time, it was noticed that the aspect ratio of the nanocones had a greater influence on decreasing the reflectivity of the samples as compared to the average density of nanostructures per unit area. The photovoltaic properties of the samples were found to be relatively similar with V_{oc} values for all the 4 samples to be around 530 mV, and fill factors obtained to be hovering around 72.5%. This implies that the effect of changing the gas ratios present in the discharge had little minimal influence on changing the electrical properties of the material. Conversely, it strongly affected the optical properties of the material in terms of reducing the amount of reflective losses on the surface.

Silicon nitride thin films were grown with ICP CVD for surface passivation. Following which, samples were annealed in a furnace at 250 ºC for 45 minutes. The EQE of the samples were measured during each stage of the fabrication process, and are shown in Figure 4(c). It is seen that there is a marked increase in the overall EQE when a thin film of silicon nitride was employed on the surface as an anti-reflection coating. Upon annealing, the EQE curve was seen to shift upwards indicating a further increment after treatment in the furnace. The overall increase in EQE is attributed to the passivation effect that the silicon nitride thin films have on the samples.

Silicon nitride has a dual purpose in enhancing the lifetime of charged carriers before recombination.[25] Trap assisted recombination processes are greatly reduced with the hydrogenated silicon nitride films terminating dangling bonds on the sample surface as well as other defects which would serve as recombination centers. The introduction of the silicon nitride thin film reduces the density of such trap states, effectively increasing the carrier lifetime, subsequently leading to higher EQE results. Silicon nitride also adds a positive static charge on the surface that adds a field effect to reduce surface

recombination velocities. As charge carriers produced in the emitter layer diffuse through the material towards the surface, the high static charge density on the surface introduced by the deposition of the silicon nitride layer repels the minority carriers away from the surface eventually causing it to drift through the junction into the layer where it is a majority carrier.

The effectiveness of this field effect in passivation of the thin films can be seen in the increase in EQE in Figure 4 (c) with the introduction of the silicon nitride films. With the dual passivation nature of the silicon nitride films, the V_{oc} and fill factor of the samples also increase.

Thereafter, it was noticed that the EQE of the samples were seen to have improved after thermal annealing in Figure 4(c). This can be ascribed to the diffusion of hydrogen and oxygen atoms in the lattice interstices, forming bonds with the silicon dangling bonds.[26] Through the repair of the lattice with thermal annealing, coupled with the enhanced passivation of dangling bonds, the overall defect and trap states present in the samples decreased. As such, Shockley-Read-Hall recombination processes are greatly minimized, which increases carrier lifetimes, resulting in an increased EQE, V_{oc} and fill factor.

4. CONCLUSION

In this work, the Integrated Plasma Photovoltaic Nanofabrication Cluster comprising the multi-chambered plasma processing facility was used to fabricate fully functional PX Si based PV cells. This facility fabricates full PV cells through dry plasma processing in a highly controlled environment, with the ability to precisely manipulate the discharge conditions. This makes it possible to obtain materials properties tailored to suit the envisaged applications. Saw tooth damage is removed through reactive ion etching with O_2 + SF_6 feedstocks, before the simultaneous formation of a p-n junction together with texturing of nanocones on the surface, obtained with an Ar + H_2 discharge. Electrical contacts are then deposited

through RF magnetron sputtering with Ar feedstock and an aluminum disc as a target. Surfaces are passivated with silicon nitride thin films through ICP assisted chemical vapor deposition with SiH_4 + N_2 and H_2 as feedstock. The discharges are uniform which leads to homogeneous processing over the entire surface of the PX Si wafers, offering potential for scaling up for industrial manufacturing. Our process is scalable and compatible with the established PV manufacturing processes. This work demonstrates the capability of an integrated plasma processing facility that offers high throughput fabrication of PV cells which has the potential of lowering costs, reagents required, and eliminating environmental issues stemming from toxic byproducts from manufacturing processes as well as time required for large scale uniform fabrication of high-efficiency, commercially-viable photovoltaic solar cells.

REFERENCES

[1] G. N. Tiwari, S. Dubey, Fundamentals of photovoltaic modules and their applications, Royal Society of Chemistry, **2010**.

[2] S. Hegedus, A. Luque, Handbook of photovoltaic science and engineering, Wiley, **2011**.

[3] N. L. Panwar, S. C. Kaushik, S. Kothari, *Renew. Sust. Energ. Rev.* **2011**, 15, 1513.

[4] M. Hightower, S. A. Pierce, *Nature* **2008**, 452, 285.

[5] S. Young, *Nature* **2001**, 414, 487.

[6] J. A. Bragagnolo, B. Sopori, E. Eser, T. Hashimoto, I. Sugiyama, Production technology for passivation of polycrystalline silicon solar cells, *Proceedings of the 12th Workshop on Crystalline Silicon Solar Cell Materials and Processes*, **2002**, 300.

[7] K.-H. Yang, J.-Y. Yang, *Sol. Energ.* **2009**, 83, 2050.

[8] L. Zhao, Y. H. Zuo, C. L. Zhou, H. L. Li, H. W. Diao, W. J. Wang, *Sol. Energ.* **2010**, 84, 110.

[9] B. Liu, *Energy Procedia* **2013**, 38, 289.

[10] I. Pinter, A. Abdulhadi, Z. Makaró, N. Khanh, M. Ádám, I. Bársony, J. Poortmans, S. Sivoththaman, H.-Z. Song, G. Adriaenssens, *Appl. Surf. Sci.* **1999**, 138, 224.

[11] J. Shao, E. C. Jones, N. W. Cheung, *Surf. Coat. Technol.* **1997**, 93, 254.

[12] A. F. Tasch, S. K. Banerjee, *Nucl. Instrum.* **1996**, 112, 177.

[13] O. O. Awadelkarim, Y. Z. Wang, *Microelectron. Eng.* **1999**, 45, 299.

[14] K. Miki, K. Sakamoto, T. Sakamoto, *Surf Sci.* **1998**, 406, 312.

[15] S. Q. Xiao, S. Xu, *J. Phys. D-Appl. Phys.* **2011**, 44, 12.

[16] K. Ostrikov, S. Xu, Plasma-aided nanofabrication: from plasma sources to nanoassembly, John Wiley & Sons, **2007**.

[17] S. Q. Xiao, S. Xu, K. Ostrikov, Mater. Sci. Eng., R **2014**, 78, 1.

[18] S. Xu, S. Huang, I. Levchenko, H. Zhou, D. Wei, S. Xiao, L. Xu, W. Yan, K. Ostrikov, *Adv. Energ. Mater.* **2011**, 1, 373.

[19] H. P. Zhou, L. X. Xu, S. Xu, S. Y. Huang, D. Y. Wei, S. Q. Xiao, W. S. Yan, M. Xu, *J. Phys. D-Appl. Phys.* **2010**, 43, 7.

[20] I. B. Denysenko, S. Xu, J. D. Long, P. P. Rutkevych, N. A. Azarenkov, K. Ostrikov, *J. Appl. Phys.* **2004**, 95, 2713.

[21] Z. Sun, S. Xu, K. N. Ostrikov, *Diamond Relat. Mater.* **2002**, 11, 92.

[22] W. S. Yan, T. M. Ong, H. P. Zhou, S. Xu, *Thin Solid Films* **2012**, 520, 6900.

[23] M. Algasinger, J. Paye, F. Werner, J. Schmidt, M. S. Brandt, M. Stutzmann, S. Koynov, *Adv. Energ. Mater.* **2013**, 3, 1068.

[24] C. J. Mogab, A. C. Adams, D. L. Flamm, *J. Appl. Phys.* **1978**, 49, 3796.

[25] S. Xu, X. Zhang, Y. Li, S. Xiong, X. Geng, Y. Zhao, *Thin Solid Films* **2011**, 520, 694.

[26] K. Ostrikov, E. C. Neyts, M. Meyyappan, *Adv. Phys.* **2013**, 62, 113.

FIGURES

Figure for the graphical abstract

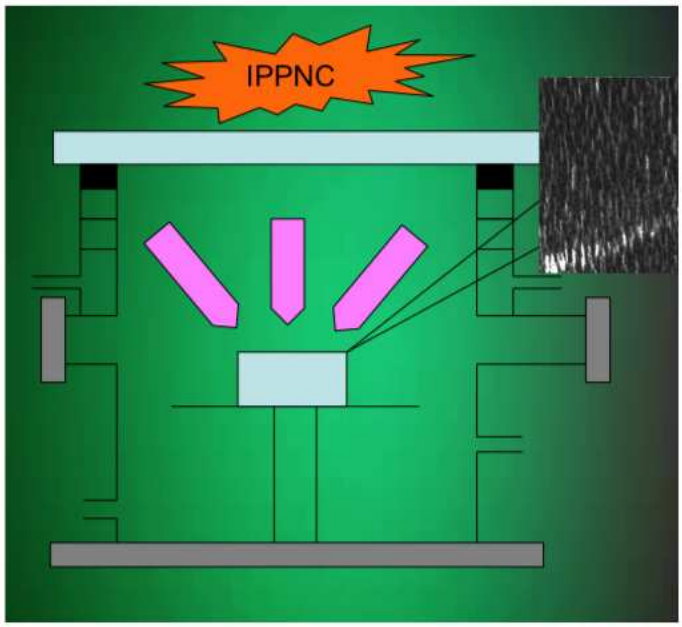

Figure 1

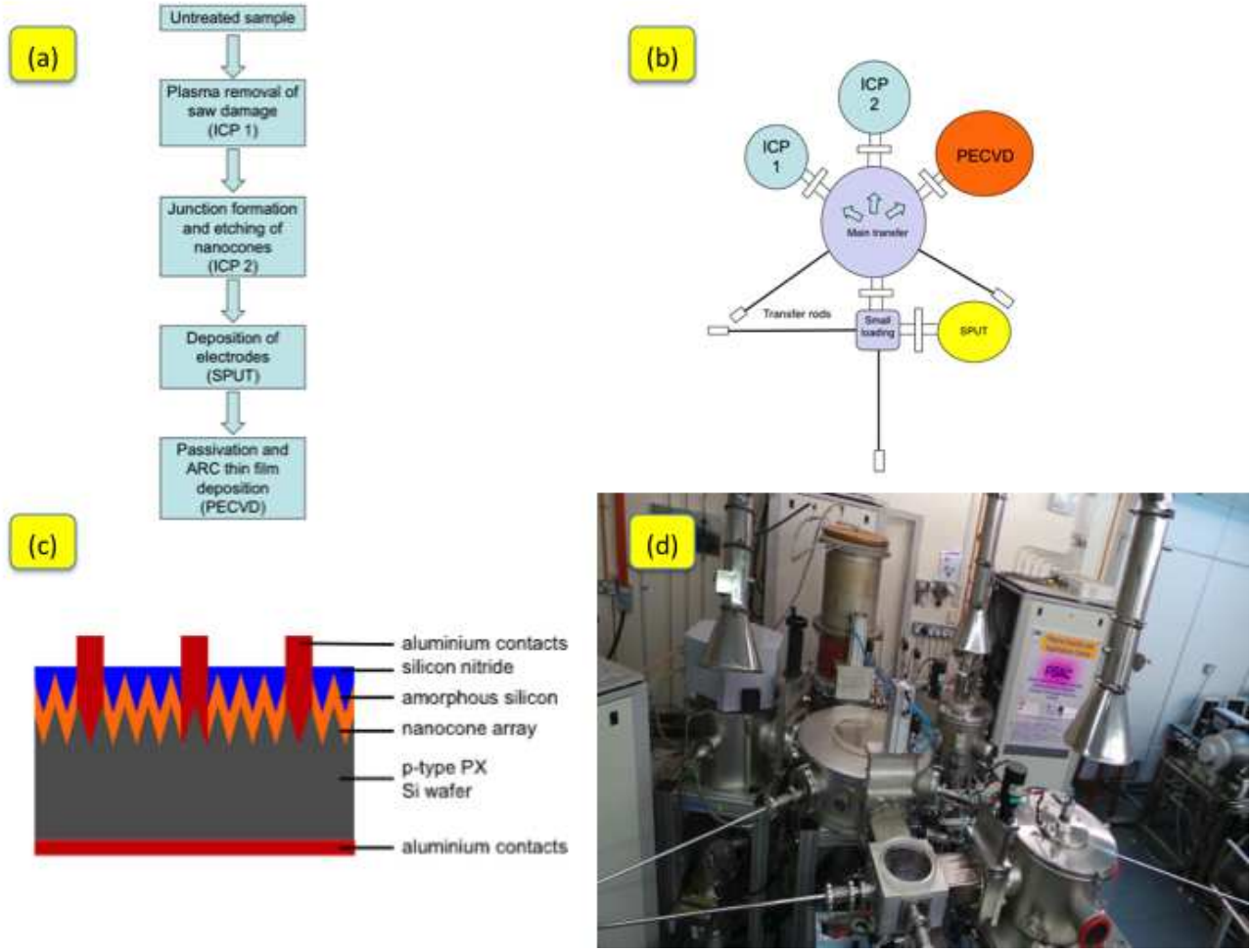

Fig. 1. Process flow for the fabrication of PX-Si nanocone PV cells (a). The schematic set up for the Integrated Plasma Photovoltaic Nanofabrication Cluster (b). Schematic design of a typical PX-Si nanocone PV cell fabricated in this work (c). Photograph of the IPPNC (d).

Figure 2

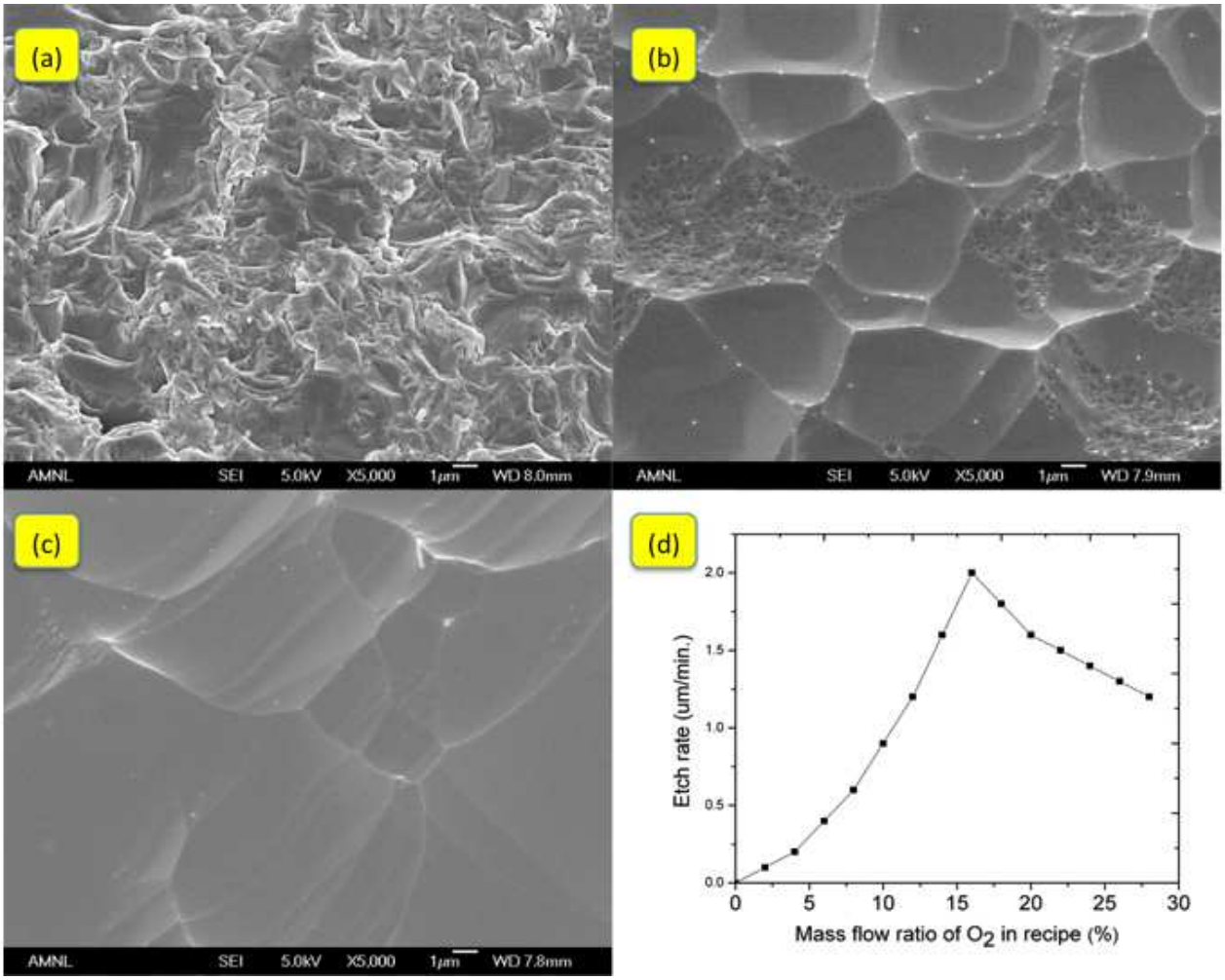

Fig. 2. Tilted SEM micrographs of bare p-type silicon wafer with saw damage (a), after SF_6 + O_2 etching with O_2 mass flow at 6% (b), and with O_2 mass flow at 16% (c). Etch rates shown as a function of O_2 mass flow (d).

Figure 3

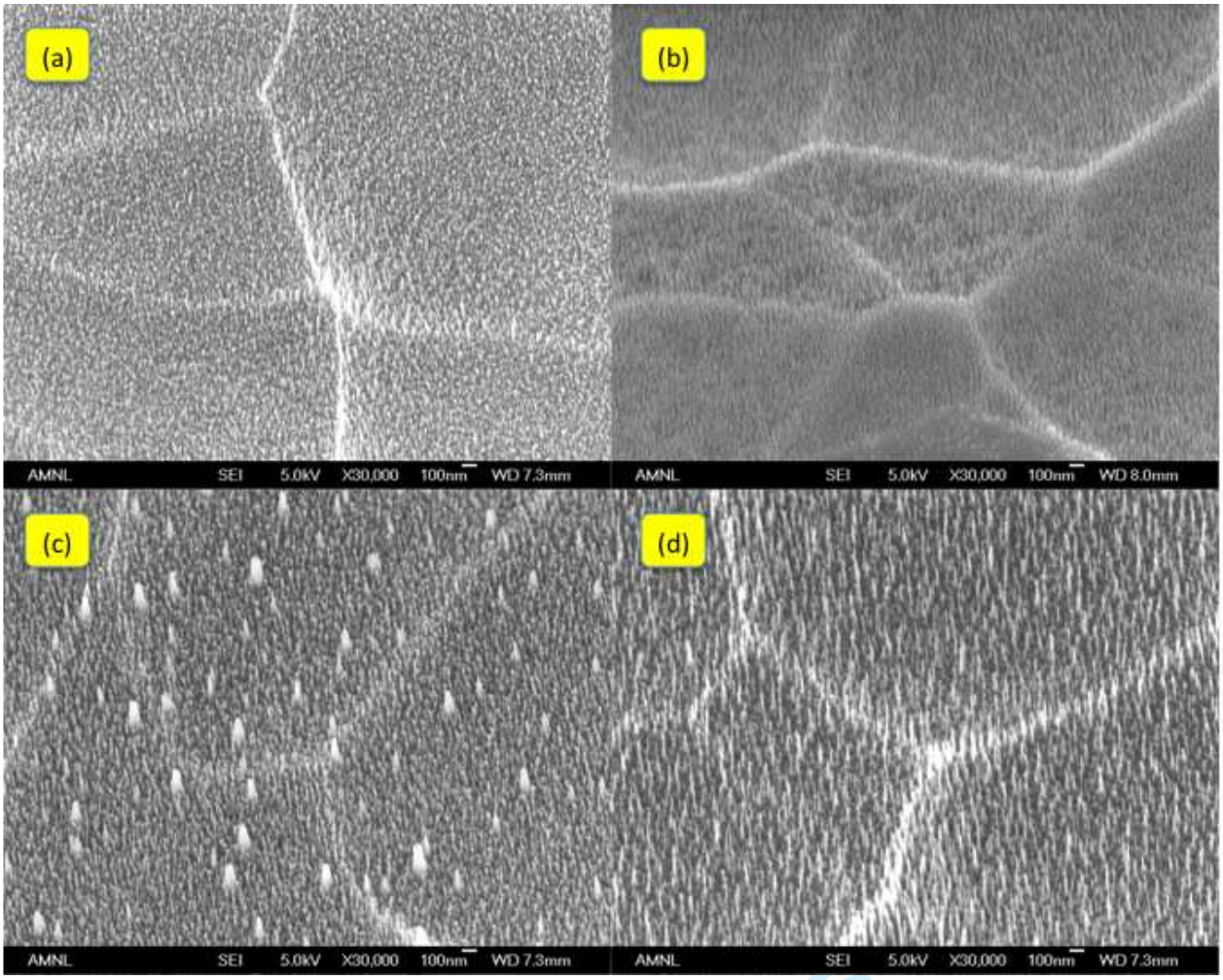

Fig. 3. Tilted SEM micrographs of silicon nanocones with 0.10 H_2/Ar ratio (a), 0.20 H_2/Ar ratio (b), 0.30 H_2/Ar ratio (c), and 0.40 H_2/Ar ratio (d) giving the best H-FWHM of 1:5.

Figure 4

(a)

Sample	Sample treatment	Reflectivity (%)
1	Bare wafer with plasma removal of saw damage	> 30
2	Sample 1 with etched silicon nanocones	2.0
3	Sample 2 with amorphous silicon for passivation	1.8
4	Sample 3 with silicon nitride as an ARC	< 1.8

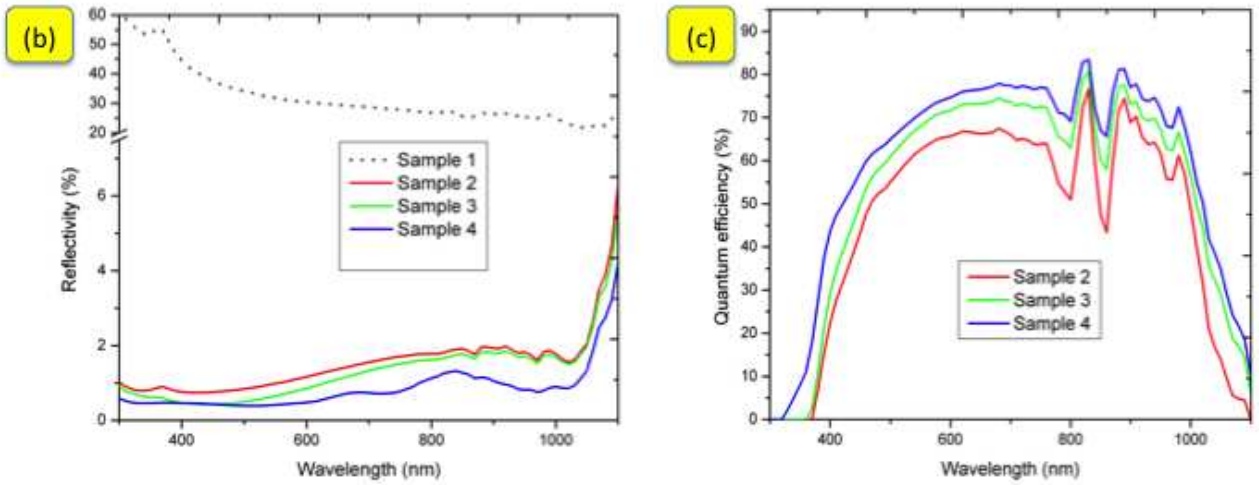

Fig. 4. PV characterization profiles of 4 samples characterized at different stages of processing (a), the reflectance spectra of the mentioned samples are given in (b), and the EQE of the samples are shown in (c).